Mon. Not. R. Astron. Soc. **270**, 173–177 (1994)

Observations of interaction between cluster gas and the radio lobes of Cygnus A

C. L. Carilli,[1] R. A. Perley[2] and D. E. Harris[3]
[1] *Leiden Observatory, Postbus 9513, 2300 RA, Leiden, The Netherlands*
[2] *National Radio Astronomy Observatory, PO Box O, Socorro, NM 87801, USA*
[3] *Harvard–Smithsonian Center for Astrophysics, 60 Garden Street, Cambridge, MA 02138, USA*

Accepted 1994 April 20. Received 1994 April 15

ABSTRACT
We present an X-ray observation of the powerful radio galaxy Cygnus A using the *ROSAT* High Resolution Imager. This observation reveals clear signatures of hydrodynamic modification of the cluster gas by the jets and lobes of the radio source. There are clear deficits of X-ray surface brightness coincident with the inner radio lobes. Such deficits suggest that the thermal cluster gas is effectively excluded from the radio lobes. Likewise, there are knots of excess X-ray emission along the edges of the radio lobes, corresponding to emission by the displaced intracluster medium (ICM). These features can be explained in the context of the jet model for the hydrodynamic evolution of the radio-emitting lobes of a powerful radio source in the centre of a dense X-ray cluster. These observations provide strong support for the basic jet model for powerful radio galaxies.

Key words: hydrodynamics – galaxies: active – galaxies: clusters: individual: Cygnus A – intergalactic medium – galaxies: jets – X-rays: galaxies.

1 INTRODUCTION

Our understanding of the formation and evolution of the characteristic components of high-luminosity extragalactic radio sources follows the models first published by Blandford & Rees (1974) and Scheuer (1974). Radio spectral studies of Cygnus A (Carilli et al. 1991) and other powerful radio galaxies (Alexander & Leahy 1987), and numerical simulations (cf. Norman et al. 1982; Clarke 1990) strongly support the standard model in which the lobes expand outwards into a cavity driven into the external medium by a supersonic, probably relativistic jet originating within the nucleus of the 'host' optical galaxy. Theory, numerical simulations, and observations all agree that the radio lobes efficiently displace the external medium, and are filled largely with relativistic jet gas which has passed through a strong shock which terminates the jet and which is identified with the 'hotspots' ubiquitously found in high-luminosity radio galaxies. Unfortunately, radio observations alone cannot give model-free estimates of such critical physical parameters as the density or the expansion speed of the lobes. Because the lobes appear empty of thermal material (Dreher, Carilli & Perley 1987), prospects of obtaining such information from the radio or optical observing bands appear to be very poor.

Detailed observations of the lobes and hotspots of sources such as Cygnus A indicate that these must be advancing supersonically into the thermal gas surrounding them. Thus the heads of the lobes must be preceded by a strong shock in the ICM. The density increase within this thin shocked layer must result in an enhanced X-ray emission which will be detectable by an X-ray instrument of suitable sensitivity and resolution. Further, the excavation of the thermal gas from the radio-emitting lobes must also result in detectable X-ray surface brightness changes, which will depend on the line of sight and the evolution of the displaced cluster gas. Thus detailed X-ray observations of these luminous objects should give valuable and unique information about the detailed physics (cf. Bohringer et al. 1993).

In such studies, it is clearly advantageous to observe luminous radio objects which are embedded in dense environments. The powerful radio galaxy Cygnus A, which is widely considered as the archetype of powerful radio galaxies, is the best candidate, for it is an ultraluminous radio galaxy embedded within a dense intracluster medium (Fabbiano et al. 1979; Arnaud et al. 1984, 1987) and, with a redshift of 0.057 (Baade & Minkowski 1954; Spinrad & Stauffer 1984), is located about a factor of 5 closer than the mean separation beween objects of its radio luminosity ($\sim 10^{45}$ erg s^{-1}).

This paper presents the results of a long *ROSAT* observation of Cygnus A with the High Resolution Imager (HRI) instrument. We have previously reported (Harris, Carilli & Perley 1994a) the detection of inverse Compton X-ray emission from the radio hotspots. Here we discuss the X-ray emission corresponding to the radio lobes and nearby regions. We show, in Section 2, what we believe are clear signs of hydrodynamic interaction between the lobes and cluster gas. We assume $H_0 = 75$ km s^{-1} Mpc^{-1} throughout, giving a scale of 1 arcsec ≡ 1 kpc.

2 THE X-RAY OBSERVATIONS AND ANALYSIS

We obtained a 66-ks exposure of Cygnus A with the *ROSAT* X-ray HRI (David et al., in preparation). The full exposure is composed of shorter segments taken over the period of 1991 April to 1993 April. The images from the various segments were aligned using a point source in the field. We estimate astrometric accuracy of about 2 arcsec (Harris et al. 1994a). The point response function (PRF) of the *ROSAT* HRI is discussed at length by David et al. It can be characterized as a Gaussian core with FWHM = 5.7 arcsec and low-level wings.

Fig. 1 (opposite) shows a contour representation of the X-ray image from *ROSAT*, smoothed with an 8-arcsec Gaussian, with a superposed grey-scale 327-MHz radio image with 5-arcsec resolution. The dominant X-ray structure is the cluster thermal emission, peaking on the centre of the Cygnus A galaxy. The low-brightness X-ray emission has good azimuthal symmetry at radii beyond ~45 arcsec. It is important to keep in mind that the *ROSAT* HRI image presented herein shows only the inner 100 kpc of the cluster. The *Einstein* IPC image of Cygnus A shows the diffuse cluster emission extending to radii of ≈500 kpc in all directions, and almost twice that distance to the north-west (Arnaud et al. 1984).

The *ROSAT* HRI image of Cygnus A shows a number of obvious departures from azimuthal symmetry. Most notable are two X-ray enhancements which are aligned with the radio hotspots, and which have been interpreted by Harris et al. (1994a) as synchrotron self-Compton emission (SSC) from the radio hotspots. In the high-brightness regions within ~45 arcsec of the centre, significant deviations from azimuthal symmetry are also found. In particular, concave X-ray isophotes are found over both radio lobes, indicating a deficiency of X-ray surface brightness coincident with the inner regions of these radio lobes. This effect is most obvious on the eastern lobe. Also, on both sides, but again more obviously on the east side, are found extensions, or 'arms' of X-ray emission which appear to envelop the inner parts of the radio lobes.

The effects of the radio lobes on the X-ray emission are more clearly seen after removal of the mean ('unperturbed') cluster radial surface brightness profile. Such removal was performed as follows. The cluster surface brightness profile was calculated from the observed X-ray brightness in regions chosen to avoid, as much as possible, lines of sight passing through the radio lobes. A modified King model was then fitted to the resulting radial surface brightness distribution. The radial surface brightness profile, $I(r)$, for a modified King model behaves as $I(r) = I_0 \times [1 + (r/a)^2]^{0.5-3\beta}$, and the implied density distribution is $n(r) = n_0 \times [1 + (r/a)^2]^{-3\beta/2}$ (cf. Forman & Jones 1991). The results for the observed profile and King fit are shown in Fig. 2. The parameters of the fit for the 'unperturbed' cluster profile of Cygnus A are: core radius $a = 35 \pm 5$ arcsec, central electron density $n_0 = 0.07 \pm 0.02$ cm^{-3}, for King-model index $\beta = 0.75 \pm 0.25$. This mean cluster radial surface brightness profile was then subtracted from the total-intensity image, and the resulting residual image is shown in Fig. 3.

Fig. 3 (opposite p. 175) shows clearly the cavities in the X-ray emission which are identified with the inner regions of the radio lobes, and the excess emission associated with the outer regions of the lobes. Also, the 'arms' of emission embracing the eastern lobe can be seen as bright knots of residual emission which pinch the inner regions of the eastern lobe. Residual emission can also be identified with the nucleus of the galaxy (Harris, Perley & Carilli 1994b).

Our conclusions on departures from azimuthal symmetry in the vicinity of the radio source are strengthened by comparison of the average radial profile for the two sectors that include the radio lobes with that for the two sectors that do not include the radio lobes. The mean surface brightness profile along the position angle of the radio lobes is also shown in Fig. 2. Beyond the extent of the radio source (radius >70 arcsec), the profiles are identical. Between 45 and 70 arcsec, the X-ray brightness from the lobe regions clearly exceeds that of the undisturbed cluster. Most of this excess is due to the hotspots, but there may also be a contribution from enhanced thermal emission associated with the lobe. Within 35 arcsec, a deficiency in brightness from the sectors overlying the radio lobes is seen.

The question of the existence of enhanced thermal emission in the vicinity of the outer regions of the radio lobes is an important one, but the outer regions of the lobes are confused by the non-thermal (SSC) X-ray emission from the high surface brightness radio-emitting regions themselves (Harris et al. 1994a). In order to address the question of excess thermal emission in the outer regions of the radio lobes, this non-thermal component must first be removed. Unfortunately, the current data lack the spectral information required to separate the two components. To investigate this important physical question, we have attempted to subtract the SSC emission using the following two simple morphological models. The first model assumes that the SSC emission is point-like, and associated with the dominant radio hotspot in each lobe. For this model the *ROSAT* PRF was scaled in intensity using the X-ray hotspot peak (as determined from Fig. 3), shifted to the hotspot position, and subtracted from the total-intensity image. For the western lobe the high surface brightness X-ray hotspot structure is well matched to the *ROSAT* PRF, and hence subtracts reasonably well from the image. However, even after point-source subtraction, a 'cap' of excess X-ray emission is seen around the end of the western lobe. This diffuse cap of emission can be seen in Fig. 1, where the lowest three contour levels follow closely the edges of the radio source in the outer ≈20 arcsec. This structure is essentially unchanged after point-source subtraction. The high X-ray surface brightness regions in the vicinity of the hotspot in the eastern lobe are not point-like, but show extension to the north-west of the hotspot (towards a bright ridge of radio emission along the northern edge of the eastern lobe; Harris

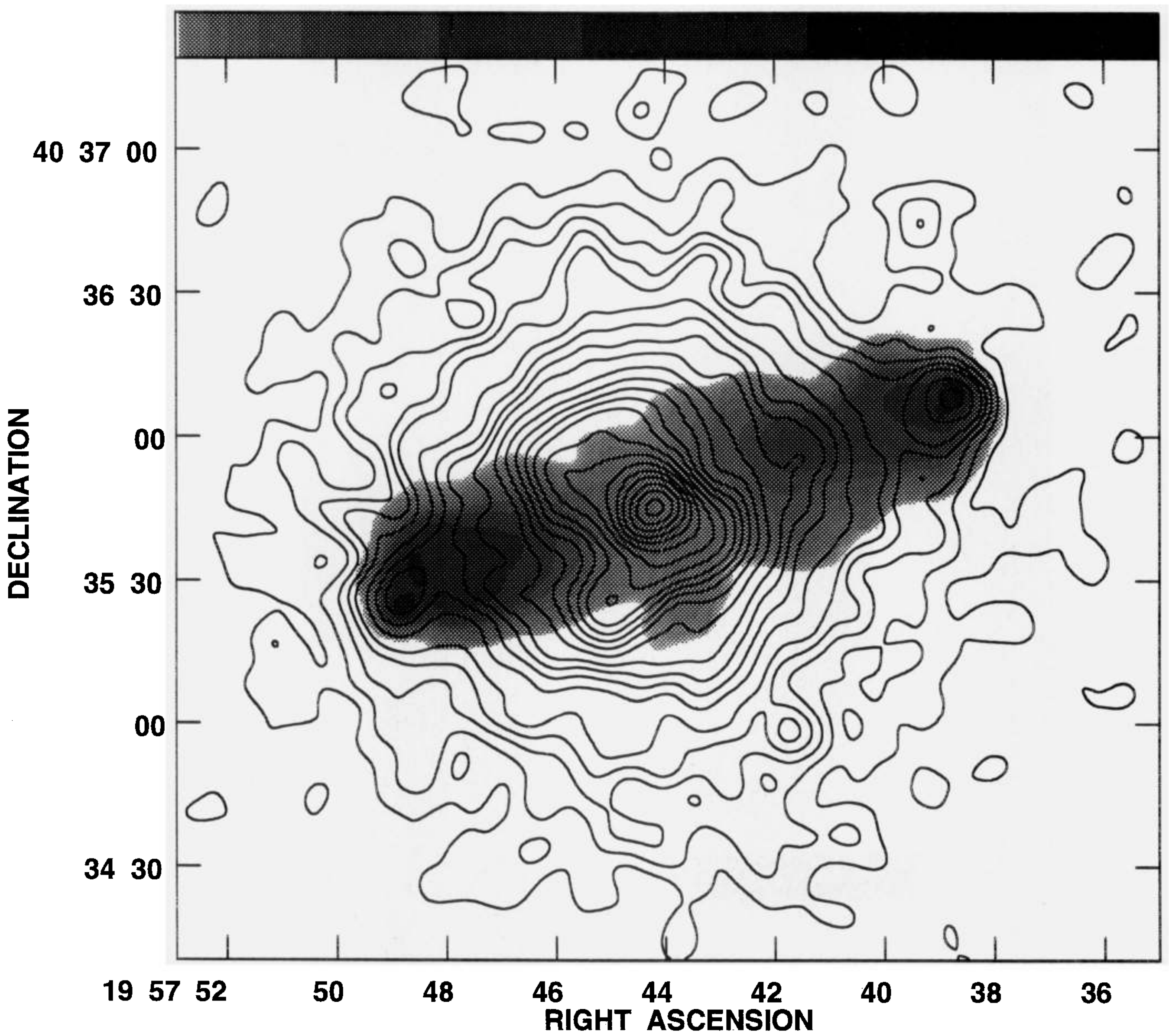

Figure 1. The grey-scale is a radio image of Cygnus A made with the VLA at 327 MHz with a resolution of 5 arcsec (Gaussian FWHM). The peak surface brightness on this image is 230 Jy beam^{-1}, and the logarithmic grey-scale ranges from 1 to 355 Jy beam^{-1}. The contours are from a 66-ks *ROSAT* HRI exposure on Cygnus A, after convolving with an 8-arcsec Gaussian. Contour levels are: 0.021 count per 0.5-arcsec pixel × (3, 4, 5, 6, 7, 9, 11, 13, 15, 18, 21, 24, 27, 30, 34, 38, 42, 46, 50, 55, 60 and 65).

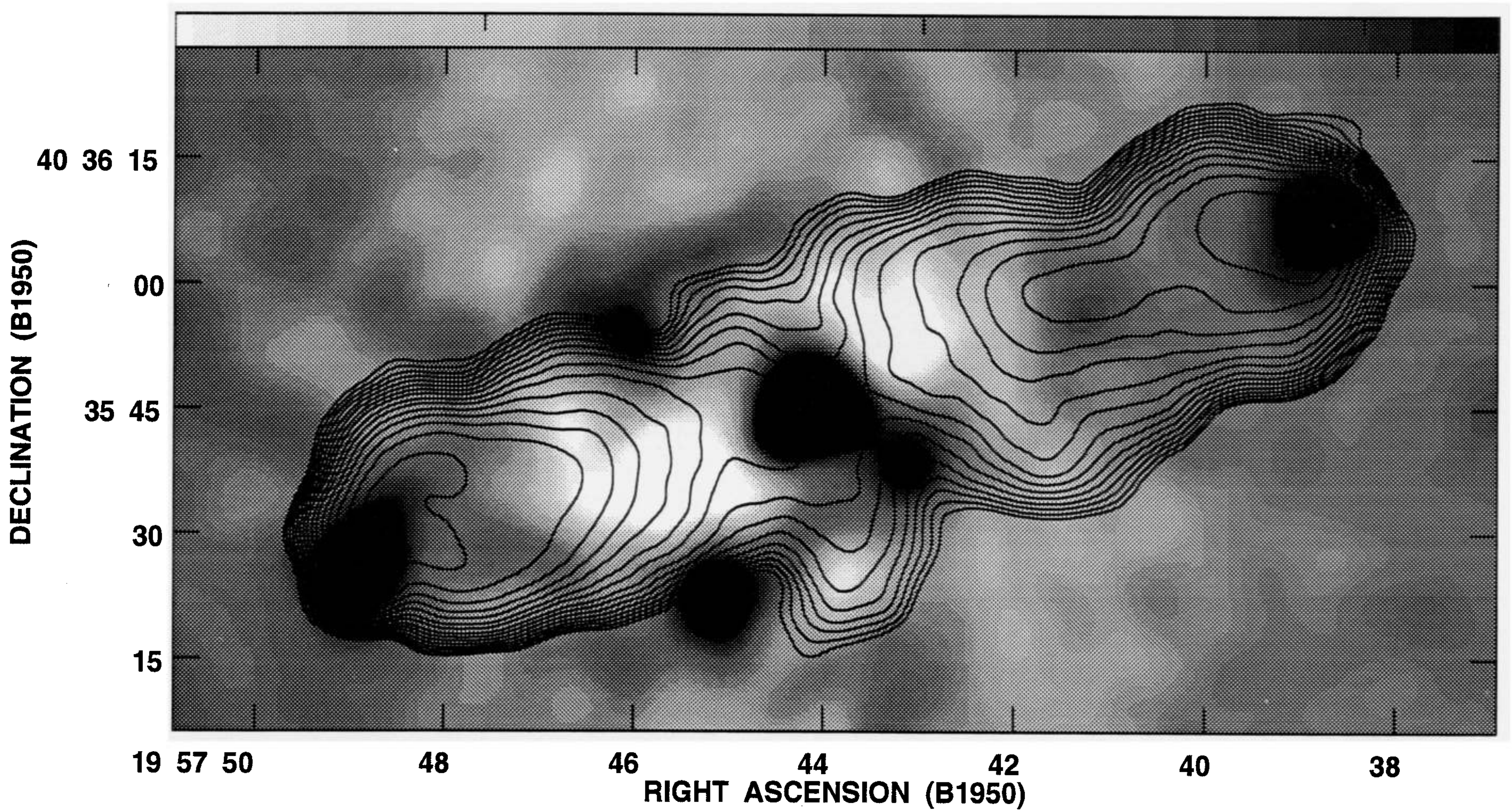

Figure 3. The grey-scale is the X-ray residual image of Cygnus A in which the smooth cluster surface brightness distribution has been subtracted. This image has been smoothed with a 7-arcsec (FWHM) Gaussian. Black denotes an excess of X-ray emission relative to the cluster mean profile, while white denotes a deficit of X-ray emission compared to the mean. The grey-scale ranges from -0.15 (white) to 0.12 (black) count per 0.5-arcsec pixel. The contours are of the same VLA image at 327 MHz as in Fig. 1. The contour levels are a geometric progression in $2^{1/2}$, which implies a factor of 2 change in surface brightness every two contours. The first level is 1 Jy beam^{-1}, and four negative levels are included.

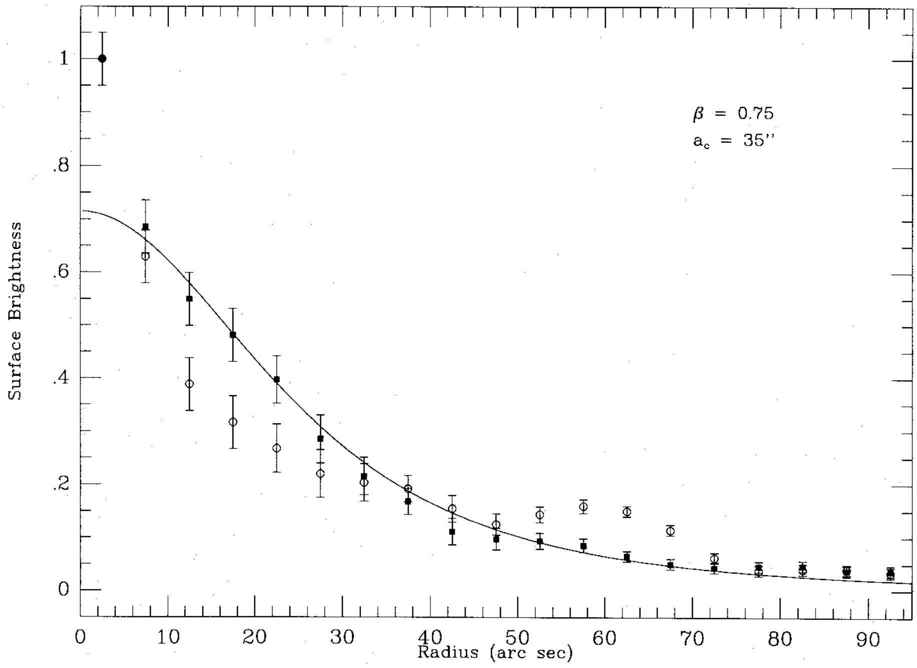

Figure 2. Radial profiles for the X-ray cluster emission in Cygnus A. The filled squares show the average profile for regions chosen to avoid, as much as possible, the radio lobes. The open circles show the average radial profile for regions along the radio lobes. The peak has been normalized to one (see Fig. 1 for the peak surface brightness in count pixel^{-1}). The error bars represent the rms scatter within the given annulus. The solid line is the best King-model fit to the off-lobe profile, using data at radii ≥ 6 arcsec.

et al. 1994a). In this case, point-source subtraction leaves obvious high surface brightness residuals at the end of the eastern lobe.

The second model assumes that the SSC X-ray emission is distributed in exactly the same way as the high-frequency radio continuum emission. For this model a radio image at 15 GHz with 0.5-arcsec resolution was convolved with the *ROSAT* PRF, and scaled as above. This model was then subtracted from the total-intensity X-ray image, and the residuals convolved as above. The result in this case is no significant residual emission associated with the outer part of the western radio lobe, i.e. this model effectively removes both the X-ray hotspot and the diffuse cap around the end of the lobe. For the eastern lobe, although more of the high surface brightness emission in the hotspot vicinity is subtracted with this model than for the simple point-source model, there is still significant residual X-ray emission associated with the outer regions of the radio lobe.

Overall, the only firm conclusion that can be made about the excess X-ray emission associated with the outer 20 arcsec or so of the radio lobes of Cygnus A is that it is not strictly point-like. Determination of the thermal contribution to this excess can only be achieved with further high-resolution X-ray observations, preferably with spectral information, such as will be possible with the *AXAF*.

3 THE X-RAY SIGNATURE OF THE HYDRODYNAMIC INTERACTION OF CLUSTER GAS AND RADIO LOBES IN CYGNUS A

The *ROSAT* HRI observations of Cygnus A show a number of significant departures from the azimuthally symmetric cluster emission. These include (A) non-thermal (SSC) emission from the radio hotspots, (B) residual emission from the nucleus, (C) deficits of X-ray surface brightness in regions coincident with the inner parts of the radio lobes, and (D) knots of excess X-ray emission along some edges of the radio lobes. Points (A) and (B) have been considered elsewhere (Harris et al. 1994a,b). Here we consider points (C) and (D), and interpret these as being the signatures of the hydrodynamic interaction between the expanding radio source and the cluster gas.

The basic physical picture for the interaction between the radio-emitting lobes and the thermal cluster gas is simply this: the supersonically advancing radio source is preceded by a bow shock in the ICM, and hence enveloped by a sheath of shocked ICM (cf. Begelman & Cioffi 1989). The two fluids (shocked ICM and radio-emitting material) meet in pressure balance along a contact discontinuity which is apparently stable to mixing (Carilli, Perley & Dreher 1988). If the jet direction is roughly constant over time, the radio lobe grows roughly as a 'cigar'-shaped cavity, with the principal active surface being associated with the high radio surface brightness regions at the head of the lobe (Begelman, Blandford & Rees 1984; Begelman & Cioffi 1989). In this model, the shocked ICM forms a thin, dense sheath in the vicinity of the heads of the lobes (since this is the location of the 'driving piston'), and a much broader, less-dense sheath in the vicinity of the tails of the radio lobes.

The continuum emissivity of a hot thermal gas is given by $\varepsilon_\nu \propto n_e^2 T^{-0.5} \exp(-h\nu/kT)$. Limiting the reception band (defined by the HRI effective area curve and the Galactic value of the column density of hydrogen in this direction) to between 0.9 and 1.7 keV, the observed flux (count rate) will be

$$f \propto n_e^2 T^{0.5} (e^{-0.9/kT} - e^{-1.7/kT}).$$

Since the density enters as the square in this equation, the increase in density across the bow shock (up to a factor of 4 relative to the ambient density for a strong shock) will be the dominant effect in most cases (see below). Considering only the effect of the density, it can be shown that, for a sheath of shocked material surrounding the excavated region, a surface brightness excess is expected for lines of sight passing through the centre of the cavity as long as the stand-off distance of the shock is $\leq 0.3\times$ the cavity width. Thus, for a thin, shocked shell surrounding an excavated region, a surface brightness increase is to be expected. If the displaced gas is more broadly distributed through a thick shell, however, as, for example, might happen if the lobe expansion has stopped and the shocked gas has time to expand and cool against the undisturbed medium, the density enhancement, even though distributed over a larger path-length, will often not be enough to offset the loss due to the empty radio source. The result in such cases will be a surface brightness *decrease* for lines of sight passing through the source. Of course, for lines of sight tangential to the radio lobes, an emission increase is always expected, as there are no excavated regions to offset the increase from the density enhancement of the shocked sheath. Qualitatively, then, as we view the source from hotspots to core, we expect an X-ray surface brightness excess in the outer parts, followed by a brightness deficiency in the inner parts and, in general, brightness enhancements along the lobe-edges.

To the above discussion must be added the effect of temperature. The emissivity function peaks at $kT = 2.6$ keV, drops exponentially for lower temperatures, and declines as $T^{-0.5}$ for higher temperatures. Arnaud et al. (1987) determined a temperature of 4 keV for the ambient gas in the Cygnus A cluster. Hence the cluster gas temperature is close to the optimum value for the *ROSAT* band, and any heating of the gas by the passage of a shock will lower the emitted energy delivered to the *ROSAT* HRI. Since the temperature jump in a strong shock is roughly proportional to M^2 (where M is the Mach number of the shock), the emissivity drop is then M^{-1}, and hence will offset significantly the emissivity enhancement due to the density increase only for very strong shocks ($M > 10$).

We consider a few rough, quantitative examples. First are the X-ray cavities coincident with the inner parts of the radio lobes. The simplest model is to assume that the lobes are just holes in the ICM, i.e. to ignore any excess emission due to the displaced gas. This will give an upper limit to the expected depth of the X-ray deficit. The emissivity profile through the cluster can be integrated using the King-model density profile, both including and excluding the lobe 'cavities', under the assumption that the source lies in the plane of the sky. Such an integration predicts an X-ray surface brightness deficit due to the presence of the radio lobe of about 40 per cent (at a radius of 20 kpc). The observed profiles shown in Fig. 2 imply a maximum deficit of about 30 per cent, although the errors allow for a range of 20 to 40 per cent. The fact that the observed deficit is comparable to the maximum value possible suggests that the transverse expansion of the shocked ICM is substantial, otherwise the emission from the shocked gas would 'fill in' the observed holes, as discussed above. Likewise, the magnitude of the observed deficit suggests that the radio lobes effectively exclude the external medium, i.e. that there is little mixing along the contact discontinuity. A similar conclusion was reached by Bohringer et al. (1993) in the case of the nearby, low-luminosity radio galaxy Perseus A.

As a second example, we consider the expected surface brightness increase due to the bow shock at the leading edge of the radio source. The pressure in the radio hotspots is about 3×10^{-9} dyn cm^{-2} (Harris et al. 1994a), while that in the unperturbed cluster gas at the hotspot radius is 1×10^{-10} dyn cm^{-2} (using the external electron density of 0.01 cm^{-3} derived from our model fitting, and a temperature of 4×10^{7} K derived by Arnaud et al. 1987). Hence the hotspots must be confined by ram pressure, and the implied Mach number is about 5. A Mach 5, non-radiative shock implies a density jump by a factor of 3.5 and a temperature jump by a factor of about 10. This produces an emissivity increase across the bow shock by a factor of about 5. We then use a bow-shock stand-off distance of 3 kpc, and assume that the shocked gas envelops the entire head of the radio lobe and that the lobes lie close to the sky plane (Carilli et al. 1988). Integration of the emissivity through the cluster (again using the King density profile), both including and excluding the shocked region, then yields an expected rise in X-ray surface brightness at the leading edge of the radio lobe by a factor of between 1.5 and 2, with the range dictated by the errors on the King-model parameters. The current data are consistent with a change in the surface brightness of the thermal emission in the vicinity of the leading edges of the lobes between 1 (i.e. no change) and 3. Again, determination of the surface brightness jump at the bow shock remains problematic due to the confusion by the non-thermal emission from the high surface brightness radio-emitting regions themselves, coupled with the finite resolution of the current image and the lack of spectral information in the current data. All of these difficulties will be overcome by the next generation of X-ray telescopes.

A final point we consider is the pressure in the various gaseous constituents in the inner regions of the cluster. The minimum energy pressure in the radio 'bridge' in Cygnus A (i.e. regions within 20 arcsec of the nucleus) is about 1×10^{-10} dyn cm^{-2}, derived using the same assumptions as in Carilli et al. (1991) and, in particular, assuming that the pressure is dominated by relativistic electrons. The pressure in the X-ray-emitting cluster gas at a radius of 20 kpc is about 5×10^{-10} dyn cm^{-2}, while that in the clumpy optical-line-emitting gas in these regions is about 8×10^{-10} dyn cm^{-2} (Carilli et al. 1989; Osterbrock 1989). Hence the pressure in the thermal gas within 20 kpc of the centre of the cluster is considerably larger than minimum energy pressures in the radio bridge. On the other hand, the observed exclusion of the cluster gas from the radio lobes in these regions dictates lobe pressures comparable to, or larger than, cluster gas pressures. One possible solution to this apparent contradiction is a significant departure from minimum energy conditions in the radio lobes. A second solution is to assume that the lobe pressure is dominated by relativistic protons (cf. Bohringer et al. 1993). Equilibration of minimum energy pressures in the radio bridge with cluster thermal gas pressures requires a ratio of the energy density in relativistic protons to that in electrons of about 20.

ACKNOWLEDGMENTS

The National Radio Astronomy Observatory is operated by Associated Universities, Inc., under cooperative agreement with the National Science Foundation. The X-ray work at SAO was supported by NASA grants NAG5-1536 and NAS5-30934. CLC acknowledges support from a NOVA research fellowship at the University of Leiden.

REFERENCES

Alexander P., Leahy J. P., 1987, MNRAS, 225, 1
Arnaud K. A., Fabian A. C., Eales S. A., Jones C., Forman W., 1984, MNRAS, 211, 981
Arnaud K. A., Johnstone R. M., Fabian A. C., Crawford C. S., Nulsen P. E., Shafer R. A., Mushotzky R. F., 1987, MNRAS, 227, 241
Baade W., Minkowski R., 1954, ApJ, 119, 206
Begelman M. C., Cioffi D. F., 1989, ApJ, 345, L21
Begelman M. C., Blandford R., Rees M., 1984, Rev. Mod. Phys., 56, 255
Blandford R., Rees M., 1974, MNRAS, 169, 395
Bohringer H., Voges W., Fabian A. C., Edge A. C., Neumann D. M., 1993, MNRAS, 264, L25
Carilli C. L., Perley R. A., Dreher J. W., 1988, ApJ, 334, L73
Carilli C. L., Dreher J. W., Conner S., Perley R. A., 1989, AJ, 98, 513
Carilli C. L., Perley R. A., Dreher J. W., Leahy J. P., 1991, ApJ, 383, 554
Clarke D. A., 1990, in Beck R., ed., Galactic and Intergalactic Magnetic Fields. Reidel, Dordrecht, p. 403
Dreher J. W., Carilli C. L., Perley R. A., 1987, ApJ, 316, 611
Fabbiano G., Doxsey R. E., Johnston M., Schwartz D. A., Schwartz J., 1979, ApJ, 230, L67
Forman W., Jones C., 1991, in Fabian A., ed., Clusters and Superclusters of Galaxies. Kluwer Academic Press, Dordrecht, p. 49
Harris D. E., Carilli C. L., Perley R. A., 1994a, Nat, 367, 713
Harris D. E., Perley R. A., Carilli C. L., 1994b, in Courvoisier T. J.-L., Blecha A., eds, Active Galactic Nuclei across the Electromagnetic Spectrum. Kluwer Academic Press, Dordrecht, in press
Norman M. L., Smarr L., Winkler K.-H., Smith M. D., 1982, A&A, 113, 285
Osterbrock D. E., 1989, Astrophysics of Gaseous Nebulae and Active Galactic Nuclei. University Science Books, Mill Valley, CA
Scheuer P. A. G., 1974, MNRAS, 166, 513
Spinrad H., Stauffer J. R., 1982, MNRAS, 200, 153